Astrophysics, Vol. 59, No. 2, June, 2016

HYSTERESIS EFFECT IN THE ACTIVITY INDICES OF THE ATMOSPHERES OF THE SUN AND SOLAR-TYPE STARS DURING THE RISING AND FALLING PHASES OF CYCLES

E. A. Bruevich and G. V. Yakunina

The hysteresis effect that shows up as a nonunique relationship among the emissions from the photosphere, chromosphere, and corona during the rising and falling phases of solar and stellar activity is analyzed. The following solar indices are analyzed and compared in different phases of the cycle: the radiative flux in the hydrogen Lyman alpha line $F_{L\alpha}$, radio emission at 10.7 cm $F_{10.7}$, the sunspot number SSN, the radiative flux in the 530.0 nm green coronal line $F_{530.3}$, the solar constant TSI, and the relative flux ratio c/w (ratio of the fluxes in the center and in the wings) for the 280 nm Mg II line. In stars with cycles, a hysteresis effect is observed between the CaII chromospheric S-activity index for stars in the Mount Wilson HK project and the photospheric flux F_{ph} for these stars.

Keywords: *Sun: activity indices, solar-type stars: HK project, activity cycles*

1. Introduction

The hysteresis effect during different levels of solar activity shows up as a nonunique relationship among the emission from the solar photosphere, chromosphere, and corona. Hysteresis in solar-earth physics has been under

P. K. Shternberg State Astronomical Institute, Moscow State University, Russia; email: red-field@yandex.ru; yakunina@sai.msu.ru

Original article submitted April 19, 2016; accepted for publication June 22, 2016. Translated from Astrofizika, Vol. 59, No. 3, pp. 413-428 (August 2016).

active study for some time [1-3]. This effect occurs in widely different manifestations of activity: from variations in the sun's short wavelength emission, to variations in its visible and radio frequency emissions. Hysteresis is observed in those cases where the state of the system being studied is determined by external conditions, not only at a given time but during earlier times, i.e., the behavior of the system over an interval of time is determined to a great extent by its prehistory. It is known that solar cycles are nonsymmetric with respect to their maxima and minima: the rise to the maximum is shorter than the fall to the minimum, and the risetime is shorter for cycles with larger amplitudes. We have studied the correlation between several indices of solar activity and $F_{10.7}$ for 21-23 cycles. [4]. It turns out that the correlation coefficient is a function of the phase of the activity cycle and it has an asymmetric time dependence during the rising and falling periods of the cycles. This fact, along with the observed time shifts between the maxima of different indices of solar activity over a single cycle, indicates the existence of hysteresis effects. In addition, the time variation of the indices during the rising and falling phases differs from one cycle to another.

The hysteresis in 7 activity indices has been studied on the basis of observations made during 1970-1990 [3]. It was found that the hysteresis is a result of the relative delay in reaching the maximum and minimum of different solar activity indices and is an important key to searching for the physical processes responsible for the variability of solar radiation at different wavelengths. The hysteresis in a pair of indices, the UV flux in the Lyman alpha line and the radio frequency flux at 10.7 cm, has been studied [5] on the basis of observations made during 1980-1990 with several Russian satellites (Prognoz 7, 8, Phobos, and Koronas-I).

Cosmic rays of galactic origin should have a constant intensity level on earth, but their interactions with the heliospheric medium cause substantial variations in the intensity of galactic cosmic rays. 11-year variations have been observed which anticorrelate with sunspot activity. The cosmic ray intensity is minimal during a sunspot maximum, but this relationship is not exact. Delays (lags) are observed, for example, between the maximum fluxes of cosmic rays and the minimum of sunspot activity for a few months. The intensity of the cosmic rays lags behind the number of sunspots, so that a hysteresis effect is observed [6,7].

The time relationship between the p-modes at frequencies measured simultaneously by the earth-based helioseismic network GONG and the MDI instrument installed on SOHO has been analyzed [8]. Several solar indices in the rising and falling branches of solar activity in the 23-rd cycle were studied at the same time. A preliminary analysis showed that the frequencies of the p-mode vary with a delay of one month from the SSN.

We have chosen the 22-nd cycle for the present study of the hysteresis effect in solar activity. The temporal evolution of solar activity in this cycle is characterized by standard behavior of the indices during the rising and falling phases, as opposed to the 23-rd cycle, which had an anomalously delayed falling phase. This paper is devoted to an analysis of the hysteresis effect in the solar activity indices during the rising and falling phases of the 22-nd cycle. We also study the hysteresis that we have observed in stars from the HK project (with stable activity cycles similar to those of the sun) between the radiative fluxes from their photospheres and chromospheres in the H and K lines of Ca II.

2. Hysteresis in the solar activity indices during the 22-nd cycle

2.1. Analysis of data from observations of the solar indices. In order to study the hysteresis effect, we have selected the index $F_{10.7}$ (the flux of radio emission at a wavelength 10.7 cm (2800 MHz)) as an objective indicator that determines the current level of the sun's activity. The flux $F_{10.7}$ is measured in sfu (solar flux units). 1 sfu corresponds to a flux of 10^{-22} W/m^2/Hz. We have analyzed several indices of solar activity: the radiative flux in the hydrogen Lyman alpha line F_L , radio emission at 10.7 cm $F_{10.7}$, the sunspot number SSN, the radiative flux in the 530.3 nm green coronal line $F_{530.3}$, the solar constant TSI, and the relative flux ratio c/w (core to wing ratio) for the 280 nm Mg II line. Here we use observational data on $F_{10.7}$, SSN, and other activity indices from the archives of the NOAA, the National Geophysical Data Center (see references in Table 1).

The relationship between the fluxes F_L and $F_{10.7}$ has been analyzed in Ref. 3, where the data correspond to 27-day sliding averages for the rising and falling phases of cycles 21-22. It turns out that in the falling phase the

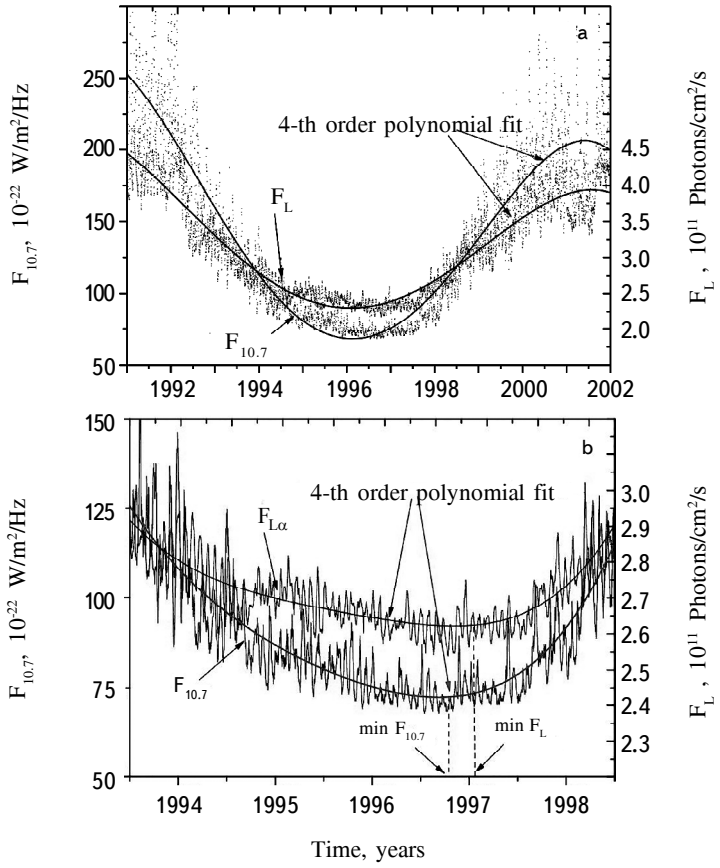

Fig. 1. (a) Time series of daily observations of sliding average values of the fluxes $F_{10.7}$ and F_L (averaged over 365 days) based on observations during the 22-nd cycle. 4-th order polynomial fits in the 22-nd cycle are shown. (b) Time series of daily observations of the sliding averages (over 365 days) of the fluxes $F_{10.7}$ and F_L separately for the minimum of the 22-nd cycle.

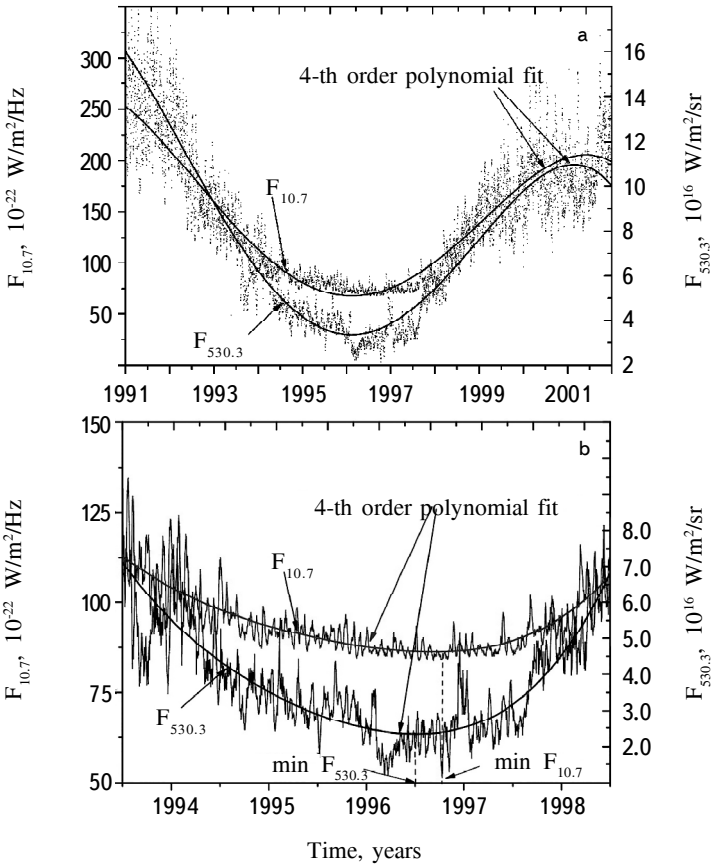

Fig. 2. (a) Time series of daily observations of sliding average values of the fluxes $F_{10.7}$ and $F_{530.3}$ (averaged over 365 days) based on observations during the 22-nd cycle. 4-th order polynomial fits in the 22-nd cycle are shown. (b) Time series of daily observations of the sliding averages (over 365 days) of the fluxes $F_{10.7}$ and $F_{530.3}$ separately for the minimum of the 22-nd cycle.

flux F_L leads the rf flux $F_{10.7}$, while in the rising phase, the rf flux $F_{10.7}$ leads the Lyman alpha flux F_L . The points in the graphs for the pairs of indices SSN-$F_{10.7}$, etc., have large scatter, which is typical of data from daily observations. The fits to the 365-day sliding averages (smooth curves) reveal a substantial hysteresis effect (20% of the average value of the index); see Fig. 1 of Ref. 3. It has been shown [9-11] that the pairs of activity indices (SSN-$F_{10.7}$) manifest a hysteresis effect: a difference in their relative variations is observed as a function of phase in the solar cycle.

Figure 1a is a plot of the sliding average of $F_{10.7}$ and F_L from the time of the maximum of cycle 22 to the time of the maximum of cycle 23. In a comparative analysis of $F_{10.7}$ and F_L during cycles 21-22 [3], it was shown that the hysteresis effect is related to the fact that the minimum of $F_{10.7}$ during cycles 21-22 sets in about 3 months earlier than that of F_L and the rising phase of $F_{10.7}$ also begins 3 months earlier. In our case, it is also clear in Fig. 1a that the relative course of the time variations in $F_{10.7}$ and F_L is nonsymmetric with respect to the minimum of

TABLE 1. Summary Data on the Solar Indices and the Times of their Minima Determined for the 22-nd Cycle

Activity index	Interval	Data source	Minimum in cycle 22	References to archival data on the internet
Flux in the Lα line, $F_{L\alpha}$ composite (daily)	1947-2015	University of Colorado	1996.9	http://lasp.colorado.edu/lisird/tss/composite_lyman_alpha.html
Flux at 10.7cm $F_{10.7}$ (daily)	1947-2016	NOAA (Penticton/ Ottawa 2800 MHz Solar flux)	1996.6	http://www.ngdc.noaa.gov/stp/space-weather/solar-data/solar-features/solar-radio/noontime-flux/penticton/penticton_observed/listings/drao_noontime-flux-observed_daily.txt
Sunspot number SSN (daily)	1818-2016	NOAA (Boulder-Sunspot Number)	1996.5	http://www.ngdc.noaa.gov/stp/space-weather/solar-data/solar-indices/sunspot-numbers/international/listings/listing_international-sunspot-numbers_daily.txt
Flux in the 530.3 nm line $F_{530.3}$ (daily)	1939-2016	NOAA (Corona-Index-Slovak Data)	1996.8	http://www.ngdc.noaa.gov/stp/space-weather/solar-data/solar-indices/solar_corona/coronal-index/slovak/
Solar constant TSI (daily)	1978-2003	NOAA (TSI Solar Composite)	1996.3	http://www.ngdc.noaa.gov/stp/space-weather/solar-data/solar-indices/total-solar-irradiance/
Mg II c/W (daily)	1978-2004 280 nm	NOAA (Mg II Composite)	1996.4	ftp://ftp.ngdc.noaa.gov/STP/SOLAR_DATA/SOLAR_UV/NOAAMgII.dat

cycles 22-23, while the rising phase of $F_{10.7}$, as in Ref. 3, begins earlier than for $F_{10.7}$ and F_L . This effect [3] is a consequence of a hysteresis between $F_{10.7}$ and F_L . Figure 1b shows separate plots for the minima in the 22-nd cycle. It is clear that the minima for the sliding averages of the fluxes $F_{10.7}$ and F_L occur at different times, roughly 3 months earlier for $F_{10.7}$. Our comparative analysis of the observed fluxes $F_{10.7}$ and F_L is mainly consistent with Ref. 3. The differences are related to the fact that uniform data on F_L from the SME satellite were used in Ref. 3, while we use composite F_L covering a wider time range (see Table 1).

In Fig. 2a, we can see the time variation of the fluxes $F_{10.7}$ and $F_{530.3}$ for the period from the maximum of cycle

22 through the maximum of cycle 23. The time dependences of $F_{10.7}$ and $F_{530.3}$ are clearly nonsymmetric in the rising and falling phases of the cycle; this shows up more strongly than for the fluxes in Fig. 1. As we shall show below, the hysteresis effect for this pair of indices is expressed more significantly. Figure 2b shows the period of the maximum of cycle 22 separately. As in Fig. 2a, one can see the asymmetry of the flux curves and the difference in the times of the minima of the fluxes $F_{10.7}$ and $F_{530.3}$. The onset times of the minima for the indices we have studied are noted in Figs. 1b and 2b, and are listed in Table 1. It can be seen, for example, that the minimum for SSN set in roughly a month earlier than for $F_{10.7}$ and 4 months earlier than the minimum for F_L .

2.2. Analysis of pairs of activity indices. We have analyzed data on the rise and fall during activity cycle 22 for 6 pairs of solar activity indices from Table 1.

Figure 3a shows the comparative variations in the daily SSN as a function of $F_{10.7}$ during cycle 22. The smooth curves are polynomial regression fits during the rising and falling phases of the solar cycle calculated for daily

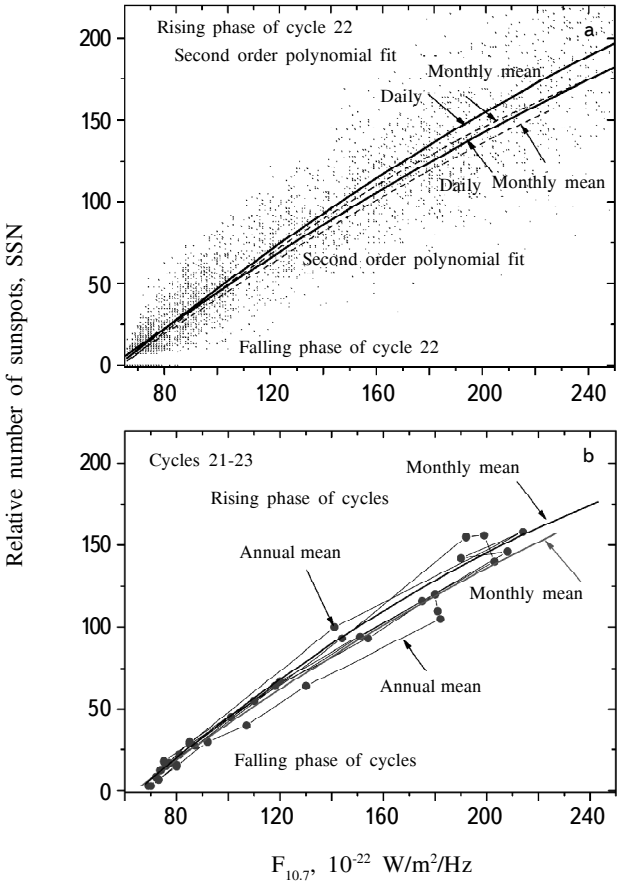

Fig. 3. Hysteresis effect for daily values of SSN as a function of $F_{10.7}$ (a) and for monthly mean and yearly averaged values of SSN as functions of $F_{10.7}$ (b).

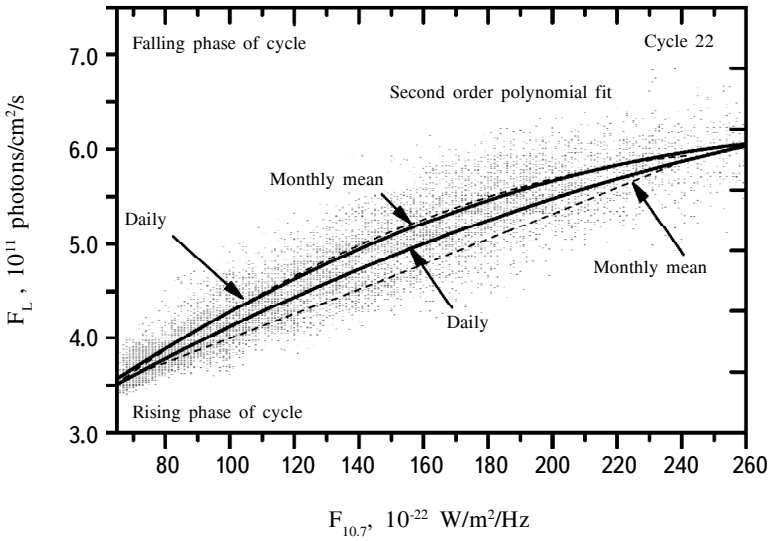

Fig. 4. Hysteresis effect for daily values of $F_{L\alpha}$ as a function of $F_{10.7}$.

observational data. For comparison, Fig. 3a also shows the mean monthly values of SSN as a function of $F_{10.7}$ during cycle 22 as dashed curves. Here we study the hysteresis effect in the solar indices using second order polynomials. Using higher order polynomials is not appropriate since the corresponding terms in the regression equations are negligibly small. This is confirmed by estimates of the residual sum of squares (RSS), defined as the sum of the squares of the deviations of the predicted values from the real empirical data. The RSS is a measure of the discrepancy between the data and the model for the estimates. A small value of RSS indicates closeness of the model and the data. RSS is used as a criterion for optimal choices of the parameters and of the model. In our case, RSS is minimal when second order polynomials are used to fit the dependence of the activity indices on $F_{10.7}$. It is clear that during the rising and falling phases of the cycle there is a nonunique relationship between the indices owing to the time delay between minima of these indices (1 month). The maximum magnitude of the hysteresis (the largest relative deviation during the cycle) is about 15%.

Figure 3b shows the comparative variations in the yearly average SSN as a function of $F_{10.7}$, combined over the three cycles 21, 22, and 23 (circles). The hysteresis in this case has evidently increased to 25%, which is considerably greater than the magnitude of the hysteresis for the monthly mean values of the SSN-$F_{10.7}$ index pair (smooth curves in Fig. 3b).

Figure 4 shows data for the daily values of the flux F_L as a function of $F_{10.7}$ during cycle 22. The smooth curves are fits to the rising and falling phases of the solar cycle calculated for the daily observation data. The dashed curves are the fits calculated for the monthly mean data. Table 2 lists the regression coefficients for the daily values of the solar activity indices separately for the rising and falling phases in the quadratic regression of Eq. (1). The hysteresis (the largest relative deviation in the cycle) reaches 10-15% for the daily observations and roughly 10-12% for the monthly average data.

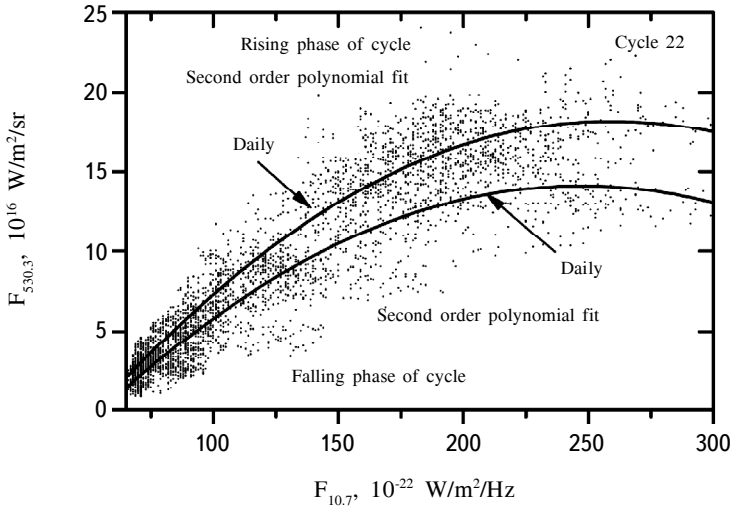

Fig. 5. Hysteresis effect for daily values of $F_{530.3}$ as a function of $F_{10.7}$.

Figure 5 shows the daily values of the flux $F_{530.3}$ as a function of $F_{10.7}$ during cycle 22. The smooth curves are fits for the rising and falling phases. The hysteresis effect shows up clearly, as in the case of the indices F_L and SSN, and the hysteresis reaches a magnitude of roughly 20%.

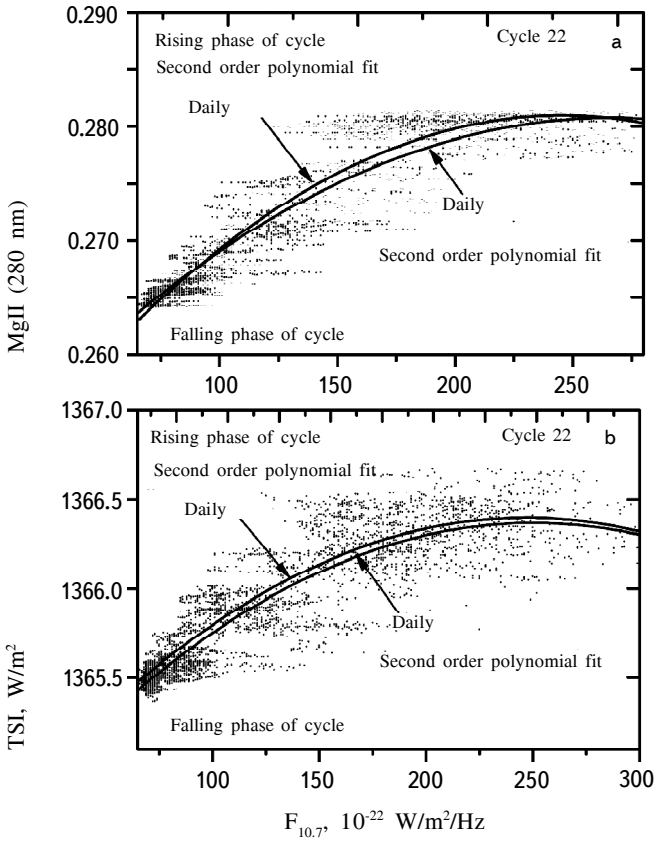

Fig. 6. Hysteresis effect for daily series of observations of indices as a function of $F_{10.7}$: MgII 280 nm c/w (a) and TSI (b).

Figure 6 shows plots of the daily data for the indices MgII c/w and TSI as functions of $F_{10.7}$. The hysteresis effect is insignificant for MgII c/w and TSI because the relative variations in the latter index during the activity cycles are very small, no more than a tenth of a percent. The quadratic fits shown in Figs. 3-6 for all the activity indices (AI) in the rising and falling phases are given by the equation

$$AI = A + C_1 F_{10.7} + C_2 F_{10.7}^2 , \quad (1)$$

where A, C_1, and C_2 are the polynomial regression coefficients listed in Table 2.

The regression coefficients from Table 2 can be used to predict the magnitude of the solar activity indices in real time, since the flux $F_{10.7}$ is determined daily. As for the rising and falling phases of the activity cycle, it is possible to improve the accuracy of predictions of the magnitudes of the indices by taking the differences in the regression coefficients for these phases into account. It should be noted that cycle 22 was chosen as the average in terms of magnitude and duration; the regression coefficients for the other activity cycles may differ from the coefficients for cycle 22 in Table 2, but these differences are not as large as the difference between the regression coefficients for a given pair of indices in the rising and falling phases of a cycle.

3. Hysteresis in the cyclical activity of stars in the HK project

As part of the HK project at the Mount Wilson Observatory, regular observations of stars analogous to the sun have been made since 1965 through the present. The Mount Wilson S-index (CaII S-index) has become the most

TABLE 2. Coefficients for Quadratic Regression Fits to the Daily Values of the Solar Activity Indices (AI) in Cycle 22 During the Rising (R) and Falling (Decline, D) Phases

$AI \leftrightarrow F_{10.7}$	A	C_1	C_2	σA	σC_1	σC_2
$SSN \leftrightarrow F_{10.7}$, R	-87.27	1.48	-0.0014	2.85	0.04	1.27E-2
$SSN \leftrightarrow F_{10.7}$, D	61.855	-0.648	0.005	0.848	0.0170	7.30E-5
$TSI \leftrightarrow F_{10.7}$, R	1364.7	0.0138	-2.79E-5	0.0223	3.14E-4	9.8E-7
$TSI \leftrightarrow F_{10.7}$, D	1364.7	2.25E-4	-4.23E-7	0.023	4.36E-6	1.40E-8
$F_{L\alpha} \leftrightarrow F_{10.7}$, R	2.142	0.024	-4.15E-5	0.074	0.0011	3.3E-6
$F_{L\alpha} \leftrightarrow F_{10.7}$, D	1.275	0.044	-1.04E-4	0.065	9.8E-4	3.17E-6
$MgII \leftrightarrow F_{10.7}$, R	0.248	2.72E-4	-5.53E-7	2.7E-4	3.8E-6	1.18E-8
$MgII \leftrightarrow F_{10.7}$, D	0.251	2.25E-4	-4.23E-7	2.9E-4	4.36E-6	1.4E-8
$F_{530.3} \leftrightarrow F_{10.7}$,R	10.644	0.222	4.29E-4	0.225	0.0032	9.86E-6
$F_{530.3} \leftrightarrow F_{10.7}$, D	-9.334	0.19	-3.84E-4	0.289	0.0043	1.36E-5

important standard characterizing the activity of stellar atmospheres in the visible. This program has been specially developed for studying the cyclical activity of solar-type F, G, and K stars. The activity cycles of 50 stars have been reliably established by prolonged observations (more than 40 years). The combined observations of radiative fluxes and rotational periods in the HK project have made it possible to detect rotational modulation of the observed fluxes for the first time [12,13]. This means that there are nonuniformities on the surface of a star which exist and evolve over a number of periods of the star's rotation about its axis. In addition, the evolution of the rotation periods of stars clearly indicates the existence of differential rotation in these stars that are analogous to the differential rotation of the sun. Rotational modulation of the photometric emission of stars was explained in terms of effects caused by starspots for the first time in Ref. 14.

Periodograms have been calculated [12] for 111 stars in the HK project for series of observations of the CaII S-index in order to determine the periods of the cycles in the cases where a cyclical activity has been detected. The significance of the height of the highest peak in a periodogram was estimated using the false alarm probability (FAP) function. Stars with peaks were classified in the following way: if $FAP \leq 10^{-9}$ for the calculated cycle period

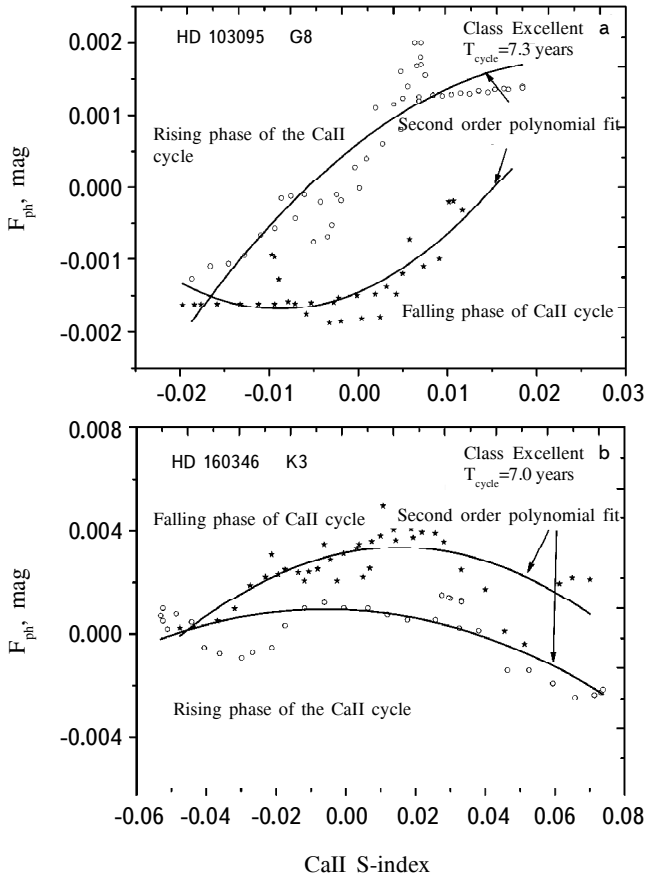

Fig. 7. Hysteresis effect in stars with activity cycles between the Ca II chromospheric S-index and the photospheric flux F_{ph}: HD 103095 (a), HD 160346 (b), HD 81809 (c), and HD 152391 (d). The hollow circles correspond to the rising phase of the cycles for the CaII S-index and the stars, to the falling phase of the cycles.

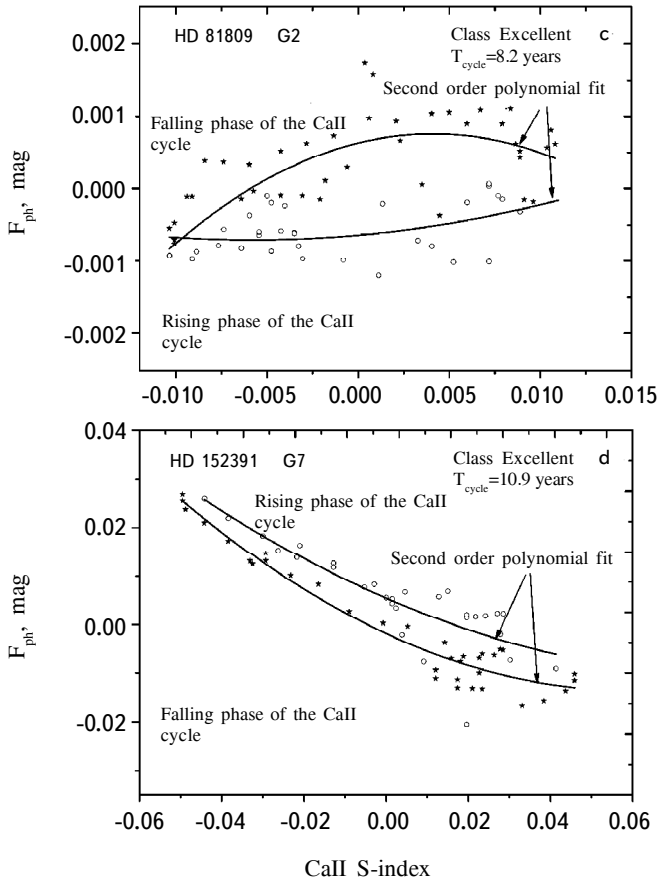

Fig. 7 (Continued)

$P_{cyc} \pm \Delta P$, then the star is assigned to the class "Excellent;" if $10^{-9} < \mathrm{FAP} \le 10^{-5}$, it is assigned to "Good;" if $10^{-5} < \mathrm{FAP} \le 10^{-2}$, it is assigned to "Fair;" and if $10^{-2} \le \mathrm{FAP} \le 10^{-1}$, it is assigned to "Poor." The periods of chromospheric activity determined by the periodogram method range from 7 to 20 years.

Photometric observations (using *b,y* Strömgren photometry) have been made for 13-20 years at the Lowell Observatory [13] in parallel with the observations of the CaII S-index at Mount Wilson for 32 stars from the same sample. In most cases, a relationship was detected between the chromospheric and photospheric fluxes of the stars: for some of the stars there is a positive correlation between these fluxes (as in the case of the sun), and for the others, the correlation is negative. Data on the variability of visible emission have been used [15] to estimate the spottedness of stars in the HK project and highly spotted stars observed at the Crimean Astrophysical Observatory [16,17] for which zonal models of the spot distribution have been constructed [18]. A close relationship was found between the spottedness and the x-ray emission power for stars with highly different levels of activity [15]. An analysis of the atmospheric activity of solar-type stars using observations from the HK project and three other extensive programs for planet searches in which the CaII S-index was determined for several thousand stars, showed that the stars in the HK project are closest to the sun in terms of their level of chromospheric and coronal emission, as well as in terms

of their cyclical activity [19].

We have chosen four stars from the HK project with the highest cyclicity classification (Excellent) based on the calculated FAP [12]: HD 103095 (a), HD 160346 (b), HD 81809 (c), and HD 152391 (d). These stars have stable cycles and belong to spectral classes G and K. The simultaneous observations of the chromospheric S-indices at Mount Wilson and the photometric fluxes F_{ph} obtained at the Lowell Observatory have been graphed in Ref. 13. We studied 3 complete activity cycles for the stars HD 103095 and HD 160346, which are characterized by cyclical activity with periods of about 7 years, and 2 complete cycles for HD 81809 and HD 152391, which have longer cycles. Using the graphical dependences from Ref. 13, we have created a data set for these 4 stars consisting of pairs of the chromospheric and photospheric activity indices averaged over 3 months (the CaII S-index and F_{ph}) separately for the rising and falling phases of the cycles.

Figure 7 shows plots of the 3-month averages of the CaII S-index as a function of F_{ph}. The smooth curves are the regression fits for the rising and falling phases of the stars' chromospheric activity cycles. The stellar index observations have also been studied using second order polynomial. The rising and falling phases of the activity cycles are defined in terms of the rise and fall in the universal CaII S-index for chromospheric activity.

It can be seen that for these stars in the "Excellent" cyclicity class, there is a hysteresis effect for the pair of indices (which characterize the chromospheric and photospheric activity) analyzed here. We note that, as the chromospheric activity increases, the activity of the photosphere does not always increase (as in the case of the sun and the stars HD 103095 and HD 81809 in Figs. 7a and 7c), but may remain roughly constant or decrease (see Figs. 7b and 7d).

4. Discussion

The above discussion shows that hysteresis effects exist for widely different manifestations of solar activity, from variations at short wavelengths to cyclical changes in the optical and radio ranges, and have also been discovered in stars with clearly distinct cyclical activity.

For the individual indices (F_L , SSN, $F_{530.3}$, and $F_{10.7}$), hysteresis effects can be explained in terms of a two-component model [20]. In the two-component model the radiative flux in line I_λ is

$$I_\lambda = B_0 + B_1\left(F^B_{10.7} - 60\right)^{2/3} + B_2\left(F_{10.7} - F^B_{10.7}\right)^{2/3}, \qquad (2)$$

where $F^B_{10.7}$ is the background flux from the unperturbed (without active regions) surface of the solar disk. $F^B_{10.7}$ at a wavelength of 10.7 cm varies from 50 to 120 sfu during an activity cycle. $(F_{10.7} - F^B_{10.7})$, which describes the contribution from active regions, also varies during a cycle. An analysis of the cyclical variations in $F_{10.7}$ has shown that, on the average, the radio frequency flux obeys an empirical regression fit of the form $F_{10.7} = a + bF^B_{10.7}$. Equation (2) for a two-component model of the variation of the flux in the line I_λ can be applied to the solar activity indices F_L , SSN, and $F_{530.3}$. The coefficients a and b characterize the contributions of the two components and vary in the

different phases of the activity cycle, as well as from cycle to cycle. This determines the nonuniform relative reduction and increase in the fluxes for the pairs of activity indices studied during different phases of the solar cycle and leads to hysteresis. The flux in weak cycles is mainly determined by the flux of background radiation, and in the strong cycles, the contribution from active regions becomes relatively more important; the hysteresis effect should be more distinct in the stronger cycles [20]. Hysteresis in the cyclical variations of the solar and stellar activity indices is most likely related to features of the structure and time evolution of solar and stellar magnetic fields, which have different effects on the various manifestations of activity in the photosphere, chromosphere, and corona.

Model calculations of the solar dynamo with the magnetic field dependence of turbulent diffusion taken into account on time scales on the order of hundreds of years also indicate a hysteresis phenomenon [21]. These calculations explain the irregular appearance of prolonged minima in the magnetic activity cycles of the sun and solar-type stars in spectral classes G and K. These calculations with a nonlinear dynamo model yield a hysteretic variation in the amplitude of the oscillations in the toroidal magnetic field B as a function of the dynamo number D, i.e., B~f(D). There are two possible regimes in the hysteresis region of this dependence: damped low-amplitude oscillations (global activity minima) and stationary cycles of relatively large amplitude (main regime). These two regimes are confirmed by observations of the sun's magnetic activity in which epochs of relatively high amplitude alternate with global minima. Fluctuations in the dynamo theory parameter in this model make it possible to reproduce the observed variability, since fluctuations in can lead to transitions between the two possible regimes in the hysteresis region of the B~f(D) dependence. Thus, the model calculations [21] show that, within a certain interval of D near a critical value D_c, there are two possible regimes: magnetic cycles with constant, relatively large amplitudes and damped low-amplitude oscillations. This corresponds to observations of solar activity in which the "ordinary" 11-year cycles alternate with epochs of global activity minima, of which the Maunder minimum is the best known [22]. Global minima also occur in other stars similar to the sun [23].

5. Conclusion

Hysteresis represents a real delay in the onset of the rise and fall in solar and stellar activity. It is an important key in searches for the physical processes responsible for variations in the emission at different wavelengths.

The hysteresis effect is typical of pairs of indices in the solar cycle, as well as for stars from the HK project, for which stable activity cycles similar to those of the sun have been discovered.

The hysteresis effect appears to be a general property of astronomical systems characterized by different manifestations of cyclical activity associated with the time evolution of their magnetic fields.

For some pairs of solar indices, the hysteresis effect shows up more strongly, but for others, it is less distinct. Here the hysteresis curves in the rising and falling phases change from cycle to cycle.

Hysteresis effects between different pairs of indices characterizing the activity of the sun and stars in different energy ranges appear to be a fundamental manifestation of magnetic activity and are related to hysteresis of the dynamo in the solar and stellar dynamo.

REFERENCES

1. K. Watanabe and H. E. Hinteregger, J. Geophys. Res. **67**, 999 (1962).
2. B. K. Ching and Y. T. Chiu, J. Atmos. Terr. Phys. **35**, 1615 (1973).
3. K. T. Bachmann and O. R. White, Solar Phys. **150**, 347 (1994).
4. E. A. Bruevich, V. V. Bruevich, and G. V. Yakunina, J. Astrophys. Astron. **35**, 1 (2014).
5. T. V. Kazachevskaya and V. V. Katyushina, Phys. Chem. Earth. **25**, 425 (2000).
6. R. P. Kane, Ann. Geophys. **25**, 2087 (2007).
7. R. P. Kane, Solar Phys. **269**, 451 (2011).
8. S. C. Tripathy, K. Jain, and K. T. Bachmann, Characteristic, Spring Meeting, abstract #SP11B-13 (2005).
9. K. L. Harvey, in R. F. Donnelly, ed., Proceedings of the Workshop on the Solar Electromagnetic Radiation Study for Solar Cycle 22, p. 113 (1992).
10. G. J. Rottman, Adv. Space Res. **8**, 53 (1988).
11. R. F. Donnelly, J. Geomag. Geoelectr. Suppl. **43**, 835 (1991).
12. S. L. Baliunas, R. F. Donahue, et al., Astrophys. J. **438**, 269 (1995).
13. G. W. Lockwood, B. A. Skiff, R. R. Radick, et al., Astrophys. J. Suppl. **171**, 260 (2007).
14. G. E. Kron, Publ. Astron. Soc. Pacif. **59**, 261 (1947).
15. E. A. Bruevich and I. Yu. Alekseev, Astrophysics, **50**, 187 (2007).
16. R. E. Gershberg, Activity of solar-type Main Sequence stars [in Russian], Astroprint, Odessa (2002).
17. I. Yu. Alekseev, Spotted low-mass stars [in Russian], Astroprint, Odessa (2001).
18. I. Yu. Alekseev and R. E. Gershberg, Astron. zh. **73**, 589 (1996).
19. E. A. Bruevich, V. V. Bruevich, and E. V. Shimanovskaya, Astrophysics, **59**, 101 (2016).
20. A. A. Nusinov, Radiophysics and Quantum Electronics. **39**, 830 (1996).
21. L. L. Kitchatinov and S. V. Olemskoy, Astron. Lett. **36**, 292 (2010).
22. Yu. I. Vitinskii, M. Kopetskii, and G. V. Kuklin, Statistics of Spotting Activity in the Sun [in Russian], Nauka, Moscow (1996).
23. S. H. Saar and S. L. Baliunas, ASP Conf. Ser. **27**, 150 (1992).